

UNDERACTUATED GRIPPER DESIGN FOR THE ASSEMBLY OF INFRASTRUCTURE IN SPACE

Niklas A. Mulsow¹ and Peter Kampmann¹

¹*DFKI Robotics Innovation Center, Robert-Hooke-Str. 1, 28359 Bremen, Germany
E-mail: niklas.mulsow@dfki.de, peter.kampmann@dfki.de*

Abstract

This paper presents the development of a concept for an adjusted self-adaptive gripper for variable manipulation tasks. Its specifications are derived from the assembly and installation of infrastructure for space applications by humans and robots working either autonomously or in collaboration. One of the core topics of the paper is the development of the kinematic for an under actuated finger, based on previous works on the self-adaptive SAMPIInG gripper system [1]. Furthermore, a suitable sensor selection for the manipulation tasks as well as their integration is presented.

1 INTRODUCTION

The interaction capability of robots with their environment is strongly determined by their grasping skills, which are mostly depending on the utilized gripper. Tasks which involve the grasping and manipulation of various objects or tools require an adaptable gripper as well as a wide range of sensors and control layers [2] [3]. Often the inspiration is taken by the human hand, which is able to grasp and manipulate objects with different sizes and shapes but in case of functionality and versatility, technological limits will be reached quickly [4]. This leads to the development of underactuated mechanisms [3].

The principle of underactuation allows the control of kinematic chains with fewer motors than there are degrees of freedom. For grippers based on underactuated designs, characteristics like dexterousness, fingertip force, weight and shape adaption are usually optimized towards special-purpose applications. Past and current applications have shown that the use of underactuated mechanisms can decrease the complexity and the weight and can also help to increase the robustness of the gripper [5] [1]. In order to determine the best grasp strategy for various tasks, a trade-off between the above mentioned key factors will be needed to develop an integrated and performant gripper.

The following sections describe the design con-

siderations taken during the development of a multi-fingered end-effector that is going to be used in conjunction with a humanoid robotic system RH5 [6] developed at the DFKI Robotics Innovation Center.

2 GRASP STRATEGY

2.1 Application Scenario

The development of the gripper described in this paper is actively involved in the project TransFIT, which is part of the space road map of the DFKI¹ RIC². The focus is on the assembly and installation of infrastructure for space applications by humans and robots either autonomously or in cooperation. Hence, the tasks for the gripper will be holding and putting together prefabricated components autonomously, in teleoperations and in collaboration with a human operator. The gripper should finally be used in the robot RH5 [6], which was developed at the DFKI in 2016. Thus, the design parameters for the structure, the weight and the grasp force should be comparable to those of a human [7]. The basic requirements are summarized in Table 1. The required dynamic grasp forces were calculated using Hesse [8] for the simultaneous movement of three arm joints with maximum velocities in case of an angular acceleration of 360 degrees per squaresecond.

2.2 Flexibility and Under Actuation

Grip stability is achieved above all by enclosing an object and an well-balanced force distribution to them. Hence, the fingers of the gripper need the capability to enclose the specified objects and to apply the grasp forces in a consistent way. The level of enclosure are determined by the degrees of freedom and maximum joint angles per finger. Inspired by human hands, three degrees of freedom per finger were determined as ideal [8]. This configuration enables a sufficient shape adaption and has the capability to enclose the object completely, like it is shown in Figure 1. To minimize

¹Deutschen Forschungszentrums für Künstliche Intelligenz

²Robotics Innovation Center

Objects	Size/Diameter	Weight
Round Material	Ø 70 mm	2,0 kg
Panels	Thickness 80 mm	1,5 kg
Tools for handover	Screwdriver, Tong, Clamp	1,5 kg
Boxes ¹	450x450x450 mm ³	5,0 kg
Gripper		Value
Size (LxWxH):		220x110x80
Weight:		< 1,5 kg
Fingers		≥ 3
Needed grasp forces ²		Value
Static Value		36,8 N
Dynamic Value		88,7 N
Maximum Value		125,5 N

¹with both hands, ²for a panel grip, $\mu = 0,2$

Table 1: Basic requires and design parameters

the effort of control and actuation, a next logical step is to extend the principle of underactuation to the hand itself in addition to individual fingers. To provide a high flexibility and the capability of

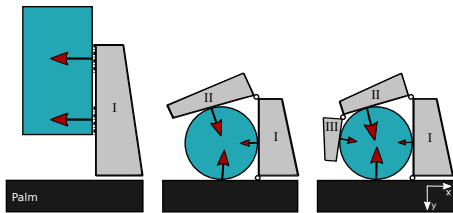


Figure 1: Grip patterns with different degrees of freedom

simple in hand manipulation, it is decided to equip each finger with an equal drive and an equal sensor suite. This reduces the costs and increases the reliability. The dexterousness of the gripper is increased by combining the finger units with auxiliary actuators, therefore an additional joint for rotating the thumb is included.

2.3 Sensor-guided manipulation

Sensors form the basis for autonomous operations. Without the capability to sense external stimuli, no internal action can be computed and executed.

According to [9] object manipulation by robots can be separated into three states: approaching an object, grasping and releasing an object. Ideally, these three states are monitored throughout the whole process using sensors. Suitable sensors are combinations of contact sensor arrays as well as near field sensing technologies.

Solutions like [10] incorporate the required sensing capabilities but are designed for the applica-

tion on robotic manipulators rather than for the integration into the limbs of end-effectors. During the design of the gripper presented here, a spatial decoupled solution between the addressed sensing modalities is aspired which allows the integration in confined limb structures.

3 FINGER KINEMATIC

To grasp objects as described in section 2.1, different types of grasps were determined (Fig.1), which shall be realized by the adaptive kinematic of the finger. Due to the known drawback of underactuated mechanisms which is the lack of performing precision grasps [5], it is decided that the kinematics has to be designed so that a parallel movement of the fingers surfaces can be achieved. The derived kinematic capabilities can be achieved by the use of tendons, deflection rollers, springs, limit stops, elastic elements or clutches in the drive train [11]. Figure 2 shows examples of kinematic models of current under actuated robotic grippers, selected from several types of state of the art grippers.

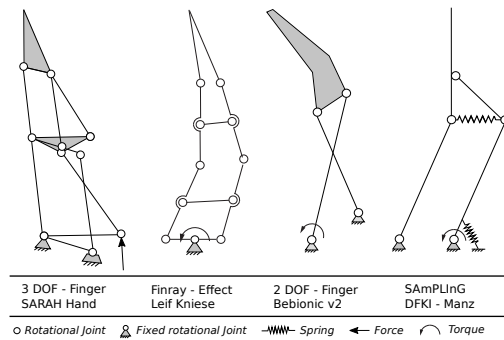


Figure 2: Example for underactuated kinematics

3.1 Concept

The SAMPLinG kinematic [1], which has been proven as a simple and robust mechanism was chosen as the initial design for the concept developed and presented here. Optimization parameters were the force introduction for a tendon drive, which leads to higher grasping forces without an additional gear. Hence, the minimization of the tendon forces will relieve the structure and allow higher safety margins. Furthermore, it will also allow to use smaller deflection rollers [12], that will be necessary to design fingers that are smaller than the ones originally used. The resulting kinematic shown in Figure 3 was derived to achieve this.

The grasp force F_G is generated by tensing the parallelogram, using a deflection roller fixed on

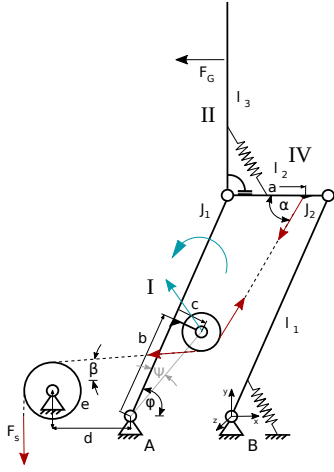


Figure 3: Simplified model of the parallel kinematic for a tendon drive

element I and the connection of the tendon with element IV. This provides a high ratio k between tension force F_s and the gained grasp force F_G (Eq: 1).

$$k = \frac{F_G}{F_s} \quad (1)$$

Another advantage of the use of a parallel kinematics is, that the force F_G will not depend on the length of L_3 [8], which is especially useful to increase the fingertip forces of the finger for a pinch grasp.

3.2 Optimization

The static description of the simplified kinematic model depicted in Figure 3 complies to the system in Equation 3. It allows the specification of geometrical dependencies of k , which are given by the distances a and b . Figure 4 describes the correlation between the parameters a , b and factor k . In case of the latter described design implementation, the distance of c was set to zero, as the influence is negligible. As it can be seen, high values for distance a have a positive effect on the force ratio k , while the relation to distance b forms a peak value. Ultimately, the highest value of k is not the only criteria of the design of the finger, as design proportions for length and thickness have to fit for the whole design. In practical applications, values for k between 0.35 and 0.70 turned out to be suitable. For the presented concept, the value of k was set to 0.45. This value is a good trade off between the resulting length and the thickness of the finger. Having identified k , the total grasp force at

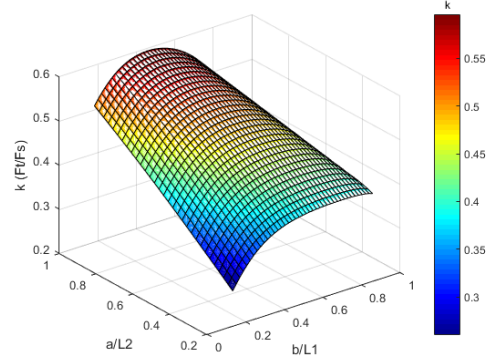


Figure 4: Relation between the geometric variables and the power ratio k of the current design (proximal angle: 90° , $e=0$, theor. max: 1)

element II F_G can be determined with:

$$F_G = k \cdot F_s \quad (2)$$

To find the maximum value for k depending on the parameters a or b , a plot of contour lines is drawn as shown in Figure 5. The effect of the opening angle φ to the correlation of k it is shown in Figure 6. For the development, assuming the angle φ to be 90 degrees is a good practice.

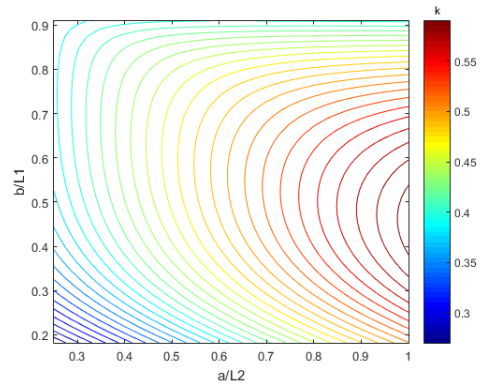


Figure 5: Contour lines for finding optimal parameters (proximal angle $\varphi: 90^\circ$)

3.3 Enhancement of the Kinematic Model

To realize the grip patterns shown in Figure 1 and to adapt the mechanism (compare Figure 3) to the application scenario, the enhanced mechanism shown in Figure 7, was developed. It increases the number of passive joints to three and enables an extended motion range in comparison to the original SAMPLinG kinematic (Fig. 2). Table 2 shows the reachable angles of movement.

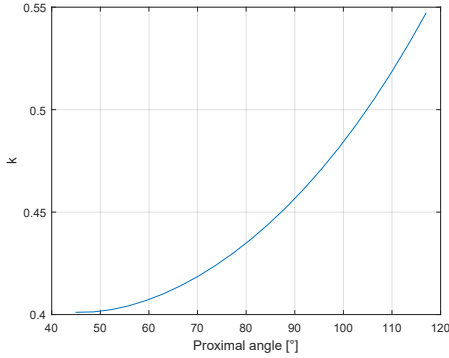


Figure 6: Grasp force depending on the opening angle

φ_1	φ_2	φ_3
90°	140°	50°

Table 2: Maximum joint angles

3.4 Stability Criterion and Force Distribution

Figure 8 shows the resulting forces and moments that can be reached by the grip of a planar body. As can be deduced from the illustration, the maximum grasp capability will be achieved when the effective point of grasping G_p^* is close to the center of gravity, since the forces caused by the moment of inertia M_{sz} can be neutralized in this way. In the ideal case, the use of the whole grasp force enables to receive the weight force of the grasped object. This is the case when G_p^* falls in line with S . When grasping objects with an edge length greater than twice the length of a finger, the center of mass is usually out of the range of the effective grasping point (Fig. 8). To minimize the distance e , there are two possibilities: extend the length of the finger or transfer the primary force contribution (Eq. 4) to the distal limb (F_{G3}), as it is the case with the human hand [8]. This kind of force distribution is also advantageous for the encompassing grip, as long as the force direction of the distal limb is pointing towards y , it causes a counterforce by the contact of the object with the palm (reconsider Fig. 1).

$$F_{total} = \sum_{i=1}^{1...n} F_{Gi} \quad (4)$$

To describe the force distribution of the successive limbs I, II and III of the developed kinematics, the factor Q was introduced, whereby: $F_{i+1} = QF_i$. With the correlation 5, the required gear reduc-

tion for the desired force distribution can be calculated, according to the geometry shown in Figure 7. For practical applications, a value around 2 for Q has been proven for various grip patterns [5].

$$\frac{Qk}{Q+1} \cdot \frac{l_3 + l_4}{r} = i_{gear} \quad (5)$$

Thierry Laliberté describes in [5] the ejection phenomenon, which occurs for underactuated fingers when the grasp stability is not given. The underactuated finger will completely close despite the contact with the object. As a result, the object will be ejected by the movement of the finger. Thus it has to be ensured that all limb grasp forces F_{Gi} for a planar grasp (Fig. 8) have to be in a positive range. This criterion will limit the maximum gear reduction i_{gear} . The maximum gear ratio for a chosen factor k can be calculated, using the equation 6.

$$k \cdot \frac{l_3 + l_4}{r} = i_{max} \quad (6)$$

3.5 Simulation Results

To verify the desired force distribution and to test the dynamic behavior during a closing sequence (Fig. 9), a simplified multibody simulation was used. The input value is the tendon force F_S in the range from 10 to 90 N in steps of 0.75 seconds. Figure 10 shows the simulated values for the given contact forces and associated joint angles. The visible spikes are due to body collisions and acceleration forces. The simulation of planar grasping has also shown compliance with the equations described in the previous sections.

4 SENSORS

Based on the requirements stated in Section 2.3 and the experiences made at the institute in previous projects, a fiber-optic measurement principle was chosen for the realisation of tactile feedback. It is of high importance that the requirements regarding power, communication as well as integration space for tactile and distance sensors are discussed already at the design phase of the gripper. With this approach, the availability of the required integration space for the manipulation sensors can be reserved. Situations, where tactile sensors have to be attached on the outside of the gripper at the end of the design or lack of tactile sensors due to unavailable integration space can be avoided.

The measurement principle was originally developed for the Canadarm of the International Space Station as well as for applications in the auto-

$$\begin{bmatrix} F_G & J_{1x} & J_{1y} & J_{2x} & J_{2y} & A_x & A_y & B_x & B_y \\ 1 & 1 & 0 & 1 & 0 & 0 & 0 & 0 & 0 \\ 0 & 0 & 1 & 0 & 1 & 0 & 0 & 0 & 0 \\ -l_2 & 0 & 0 & 0 & l_3 & 0 & 0 & 0 & 0 \\ 0 & -1 & 0 & 0 & 0 & 1 & 0 & 0 & 0 \\ 0 & 0 & -1 & 0 & 0 & 0 & 1 & 0 & 0 \\ 0 & \sin\phi_1 & -\cos\phi_1 & 0 & 0 & 0 & 0 & 0 & 0 \\ 0 & 0 & 0 & 1 & 0 & 0 & 0 & -1 & 0 \\ 0 & 0 & 0 & 0 & 1 & 0 & 0 & 0 & -1 \\ 0 & 0 & 0 & \sin\phi_1 & -\cos\phi_1 & 0 & 0 & 0 & 0 \end{bmatrix} = \begin{bmatrix} F_S \\ \cos(\alpha) \\ \sin(\alpha) \\ \sin(\alpha) \cdot a \\ \cos(\beta) - \cos(\alpha) \\ \sin(\beta) - \sin(\alpha) \\ * \\ 0 \\ 0 \\ 0 \end{bmatrix} \quad (3)$$

$$* \sin(\varphi - \psi) \cdot r \cdot \cos(\alpha) - \cos(\varphi - \psi) \cdot r \cdot \sin(\alpha) - \sin(\varphi - \psi) \cdot r \cdot \cos(\beta) + \cos(\varphi - \psi) \cdot r \cdot \sin(\beta)$$

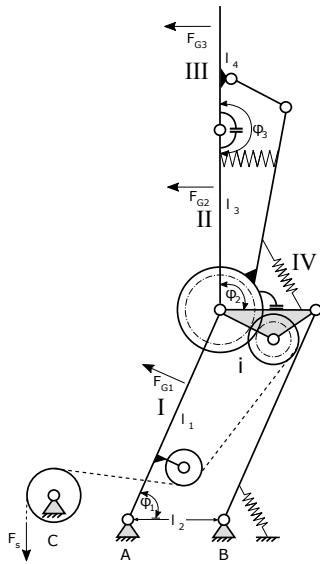


Figure 7: Final model of the underactuated finger

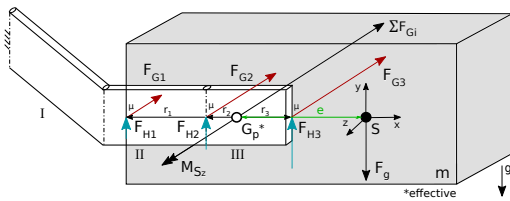


Figure 8: Force distribution for grasping of an plane object



Figure 9: Simulated closing sequence

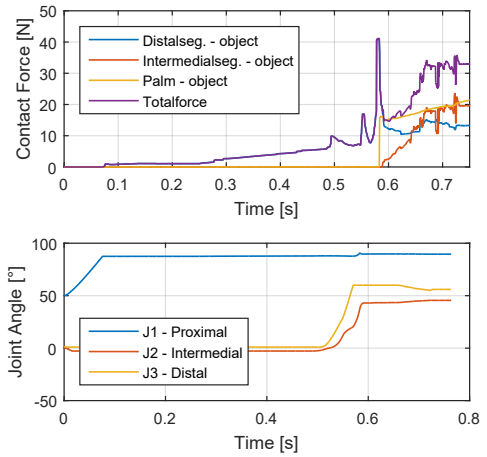


Figure 10: Contact forces and joint angles during a closing sequence for an encompassing grip

motive sector [13]. Further applications were in the domain of underwater robotics [14]. Detailed information regarding this measurement principle can be found in [15]. Within this end-effector design, small printed circuit boards (PCBs) will be designed using the discussed measurement principle that fits to the limb structure of the gripper. The PCBs comprise a light source as well as light sensing components for each sensing element of the tactile array. The measurement data is going to be converted from an analogue input to a digital one right on the same PCB using an ARM based microcontroller. The communication chain is realized using CAN Bus data transmission to a master sensor node in the palm of the robot. Relevant high-level information going to a central manipulation PC or the execution of local control loops are computed on the master sensor node.

While the contact sensors will cover the whole planar inner surface of the gripper, the near field

distance sensors are going to be placed on the finger-tips, on the outside of the gripper as well as in the palm of the gripper in a sparse configuration.

5 PROTOTYPING AND TEST RESULTS

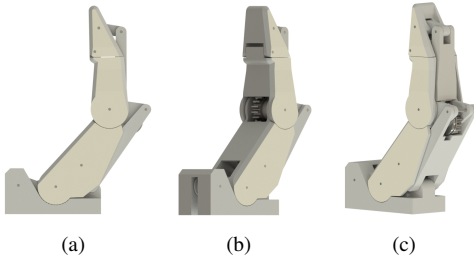


Figure 11: Renderings of the prototype finger

5.1 Mechanical Design

To prove the force distribution and the shape adaptation of the finger, a first prototype was designed (Fig. 11) and realized in SLA³ 3d-printing. The focus was on a compact design, which left space for the integration of sensors. It also protects delicate parts of the kinematics in the case of collisions. Besides forces occurring due to the tension and grasp forces, the finger was also designed to absorb high lateral forces. The kinematic limbs I,II, and III have a coverage for the inner parts that provide a robust coupling and the capability to absorb lateral overloads. The tendon force F_S in the Figures 12 was 25.0 N, which led to a finger tip force of approximately 11 Newton, depending on the opening proximal angle φ_1 . This compares to the calculated forces according to equation 2.

6 OUTLOOK

6.1 Micro Actuator Design

The mechanical design of the actuators will be derived from the DFKIx Joint [16]. This joint has passed major space qualification tests based on parameters for the LEO-Mission TET-x, like thermal-vakuum, thermal-cycling, sine- and random-vibration as well as radiation. In order to perform space operations, the design and component selection has to be adopted and modified for the usage in the final gripper. The current gear unit design for the finger actuators is depicted in Fig.

³stereolithography

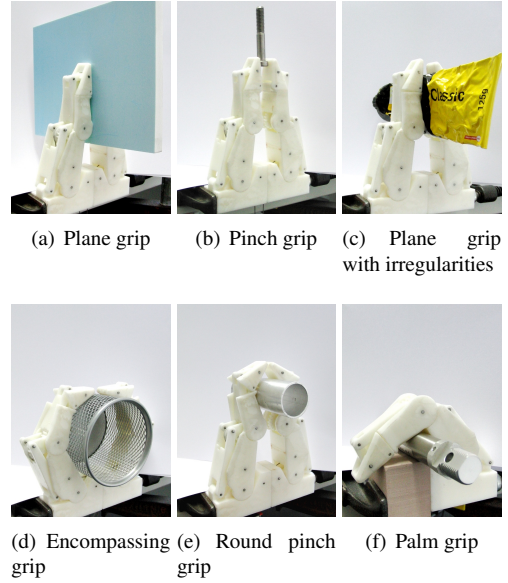


Figure 12: Variations of the shape adaptation

13. The components used are a BLDC motor Robodrives ILM 25x04, an Harmonic Drive HFUC-2A-08-100 gear, high precision SBN miniature four-point ball bearings, Hall-effect sensors for commutation and position indication, temperature sensors and a winding mechanism. The motor integration kit and the harmonic drive gear can be directly replaced by space proved hardware, while the bearing as well as the sensor equipment unit have to be adopted according to the environmental conditions. A similar design was used in the DLR's Spacehand [17]. The design was optimized towards smallest assembly space and to provide a maximum tendon force of 257 N. The overall dimensions of the mechanical micro actuator design are a length of 45 mm, a diameter of 32 mm and a weight of 87 g. There will be a finger-tip force of over 115,6 N maximum per finger in the current setup. The copper losses for holding an object with the maximum grasp force will be approximately 4 W per finger and the maximum closing speed for a fully closing sequence will be below one second.

6.2 Gripper Design

An iterative approach for designing a robotic hand is described by Grebenstein in [18]. To find out which designs will fit perfectly for the tasks, a handmade model was created and tested. The focus was on an easy and effective arrangement, to limit the control effort and also enable a mechanically robust design. In order to achieve de-



Figure 13: Micro actuator with winding mechanism

sired handle patterns with respect to the initially described application scenario four fingers were identified as an optimal configuration. To be able to grab boxes with two hands, an opposable thumb was added. This distinguishes the gripper from many industrial grippers and enables a wider range of applications, especially for the use in humanoid robots. In this configuration (see Fig. 14), the described grip pattern (Fig. 12) can be fully exploited. To keep force paths short, the micro actuators are placed directly towards the fingers. The final gripper will be equipped with five micro actuators which can apply a grasp force of more than 200 N. The weight without electronics is targeted to be under 1.4 kg.

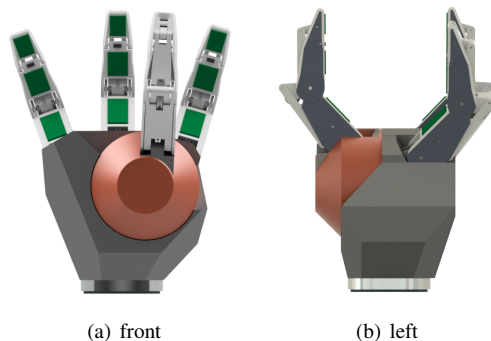


Figure 14: CAD Model of the final gripper design

6.3 Conclusion

The described finger kinematics has proved its suitability in simulation and during first practical tests by grasping various objects. The unique design of the fingers allows an outstanding high finger-tip-force, a high resistance to impacts and lateral loads as well as the integration of tactile sensors. With the developed sensor technology, it is possible to support the control of the grasping process continuously, which allows the detection of an object with near field perception and haptic measurements by touch localization. Combining the described micro actuators and the fingers,

the system can be used in multipurpose hand concepts. On the basis of future developments, the design will be examined in the interaction and tests with the humanoid RH5 robot in the context of the assembly of infrastructure in space.

7 ACKNOWLEDGEMENTS

The presented research is financed by the TransFit project which is funded by the German Federal Ministry of Economics and Technology (BMWi) according to a resolution of the German Bundestag, grant no. 50RA1701, 50RA1702 and 50RA1703.

References

- [1] Manz M, Bartsch S, Simnofske M and Kirchner F (2016) Development of a Self-Adaptive Gripper and Implementation of a Gripping Reflex to Increase the Dynamic Payload Capacity. In: *International Symposium on Robotics (ISR-2016)*.
- [2] Mason MT and Salisbury JK (1985) *Robot hands and the mechanics of manipulation*. The MIT Press. ISBN 0262132052, 978-0262132053.
- [3] Birglen L, Laliberté T and Gosselin C (2008) *Underactuated Robotic Hands*, volume 40 of *Springer Tracts in Advanced Robotics*. Springer-Verlag Berlin Heidelberg, 1 edition. ISBN 9783540774587, 3540774580.
- [4] Cutkosky MR, Howe RD, Venkataraman ST and Iberall T (1990) *Dextrous Robot Hands*. Springer-Verlag New York, 1 edition. ISBN 978-1-4613-8976-7, 978-1-4613-8974-3.
- [5] Laliberté T and Gosselin C (2001) Underactuation in space robotic hands. In: *6th International Symposium on Artificial Intelligence and Robotics and Automation in Space: i-SAIRAS*.
- [6] Peters H, Kampmann P and Simnofske M (2017) Konstruktion eines zweibeinigen humanoiden Roboters. In: *Proceedings of the 2. VDI Fachkonferenz Humanoide Roboter, VDI Fachkonferenz Humanoide Roboter*.
- [7] Rickert M (2010) *Funktionelle Normwerte und Einflussfaktoren an Unterarm und Hand gesunder männlicher Erwachsener*. Doctoral Thesis, Ludwig-Maximilians-Universität zu München, Munich.

- [8] Hesse S, Monkman J G, Stienmann R and Schunk H (2004) *Robotergriffe, Funktion, Gestaltung und Anwendung industrieller Greiftechnik*. HANSER. ISBN 3-446-22920-5.
- [9] Hesse S and Schnell G (2014) *Sensoren für die Prozess- und Fabrikautomation*. Springer Vieweg, Wiesbaden, 6 edition. ISBN 978-3-658-05866-1. doi:10.1007/978-3-658-05867-8.
- [10] Mittendorfer P and Cheng G (2011) Humanoid Multi-Modal Tactile Sensing Modules. In: *IEEE TRO - Special Issue on Robotic Sense of Touch*, pp.401–410.
- [11] Townsend W (2000) The BarrettHand grasper – programmably flexible part handling and assembly. In: *Industrial Robot: An International Journal*, 27:pp.181–188.
- [12] Rost, Arne (2013) *Untersuchung von Antrieben mit Kunststoff-Faserseilen für den Einsatz in Leichtbau-Gelenkarmrobotern*. Doctoral Thesis, Universität Stuttgart.
- [13] Reimer EM and Baldwin LH (1999) Cavity Sensor Technology for Low Cost Automotive Safety and Control Devices. In: *Air Bag Technology '99, Cobo Convention Center, Detroit*.
- [14] Kampmann P and Kirchner F (2015) Towards a fine-manipulation system with tactile feedback for deep-sea environments. In: *Robotics and Autonomous Systems*, 67:pp.115 – 121. ISSN 0921-8890. Advances in Autonomous Underwater Robotics.
- [15] Kampmann P and Kirchner F (2014) Integration of Fiber-Optic Sensor Arrays into a Multi-Modal Tactile Sensor Processing System for Robotic End-Effectors. In: *Sensors - Open Access Journal*, Special Issue Tactile Sensors and Sensing Systems(14(4)):pp.6854–6876.
- [16] Sonsalla R, Hanff H, Schöberl P, Stark T and Mulsow NA (2017) DFKI-X: A Novel, Compact and Highly Integrated Robotics Joint for Space Applications. In: *Proceedings of the 17th European Space Mechanisms and Tribology Symposium (ESMATS)*.
- [17] Chalon M, , Maier M, Bertleff W, Beyer A, Bayer R, Friedl W, Neugebauer P, Obermeier T, Sedlmayr HJ, Seitz N and Stemmer A (2015) Spacehand: a multi-fingered robotic hand for space. In: *13th Symposium on Advanced Space Technologies in Robotics and Automation (ASTRA)*.
- [18] Grebenstein M, Chalon M, Hirzinger G and Siegwart R (2010) . A Method for Hand Kinematics Designers 7 Billion Perfect Hands.